Multisensor noise attenuation with RIDNet

B. Farmani[1], M. Lesnes[1], Y. Pal[1]

[1] PGS

Summary

Before data from the multisensor streamers records are combined, it is essential to attenuate the noise from both records to ensure the creation of high-quality up- and down-going wavefields. In recent years, our industry has moved from using statistical and mathematical tools towards machine learning tools to attenuate noise in seismic data. The key motivation has been automation, consistency of output, and quality improvements. We present separate workflows for both pressure and particle motion records that use deep learning to directly attenuate the noise from the records. The heart of the workflows is a convolutional neural network called real image denoising network (RIDNet). The current workflows use a single RIDNet model with exact structure for both pressure and particle motion records to attenuate incoherent noise in the bandwidth where most of the noise exists. Both models were trained using data recorded in the field with supervised learning where the desired outputs were produced by previously developed machine learning based workflows. The new workflows have been extensively validated using records from surveys acquired with different survey geometry, water depth and sea conditions. The validation process confirms that there is no need for workflow modification or re-training of the models. Therefore, the workflows are automated and do not require user interaction.

Multisensor noise attenuation with RIDNet

Introduction

Multisensor streamers record both pressure and particle motion. The down-going wavefield has opposite polarity on pressure and particle motion records whereas the up-going wavefield has the same polarity. This feature means that recordings from these two different sensors can be combined to separate the wavefield into up- and down-going parts. Before the data from the two sensors are combined, it is essential to attenuate the noise from both records to ensure the creation of high-quality up- and down-going wavefields. In recent years, our industry has moved from using statistical and mathematical tools towards machine learning tools to attenuate noise in seismic data. The key motivation has been automation, consistency of output, and quality improvements. Machine learning applications in seismic noise attenuation can be categorized into three main groups: quality control of the noise content and signal loss (e.g., Bekara and Day, 2019); detection of noise and signal loss for automatic guiding of the noise attenuation engine (e.g., Farmani and Pedersen, 2022); and finally, direct noise attenuation (e.g., Kumar *et al*., 2022; Valenciano *et al*., 2022).

Following the work of Farmani et al. (2023), we have developed separate workflows for both pressure and particle motion records that use deep learning to directly attenuate the noise from the records. The heart of the workflows is a convolutional neural network called real image denoising network (RIDNet). RIDNet was originally designed to denoise photographic images (Anwar and Barnes, 2019). Compared to the previous machine learning based workflows we have presented; the current workflows use only a single RIDNet model with exact structure for both pressure and particle motion records to attenuate incoherent noise in the bandwidth where most of the noise exists. Therefore, the main parts of the workflows are significantly simplified and are very similar for both types of the records. Other types of noise and incoherent noise outside the RIDNet application bandwidth are attenuated by the other processes in the workflows.

Methodology

Incoherent noise attenuation on both pressure and particle motion records in the bandwidth of interest is performed using a network based on RIDNet architecture. Figure 1 shows the RIDNet network architecture. RIDNet is a modular network comprising three main modules: feature extraction, feature learning residual module, and reconstruction. In the first part of the network, features are extracted using a 2D convolutional layer. These features are then passed to a sequence of modules called enhancement attention modules (EAM). EAM branches the input features and passes them through two dilated 2D convolutions. Features are further passed through some 2D convolutions and local skip connections. By using dilation and local skip connections, the network can learn both low and high frequency features in the input data. The output of the last EAM is passed to a 2D convolutional layer to reconstruct the noise with opposite polarity. Finally, the reconstructed noise is added back to the input and the final output is generated. We used supervised learning to train the models. To create a generic and global model that can perform well on any unseen data without re-training, it is important to include a variety of signal and noise in the training dataset. We also found it beneficial to train the models with consistent noise attenuation performance regardless of the noise level in the input data. If training datasets are prepared by any human interactions, there will be inconsistency and bias in the level of the noise attenuated based on the judgment of the geophysicists. In the absence of any alternative solutions, it is of course possible to use such data for the training. However, how generic the performance of the trained models will be, depends on the consistency of the model outputs used in training.

To train the RIDNet model for noise attenuation of particle motion data, we used noise attenuated data from the workflow previously proposed by Farmani et al. (2023). In their proposed workflow, two RIDNet models are used to attenuate the noise and an addback flow in the curvelet domain is used to recover local signal loss if necessary. After extensive validation of their workflow and its application in production processing, a large body of noise attenuated data with consistent noise attenuation was available. We selected a subset of data including 1.6 million tiles from the available data and trained a single RIDNet model. Our training could reach peak signal-to-noise ratio (PSNR) of 37.04 on validation data. The new model performed as well as the previous workflow on the available data and performed equally well on new data. Our particle motion RIDNet model targets particle motion noise in frequency band 19-95 Hz. FX filters are used to attenuate the noise at frequencies outside that frequency range. Linear coherent noise is supressed using FK filters in the workflow.

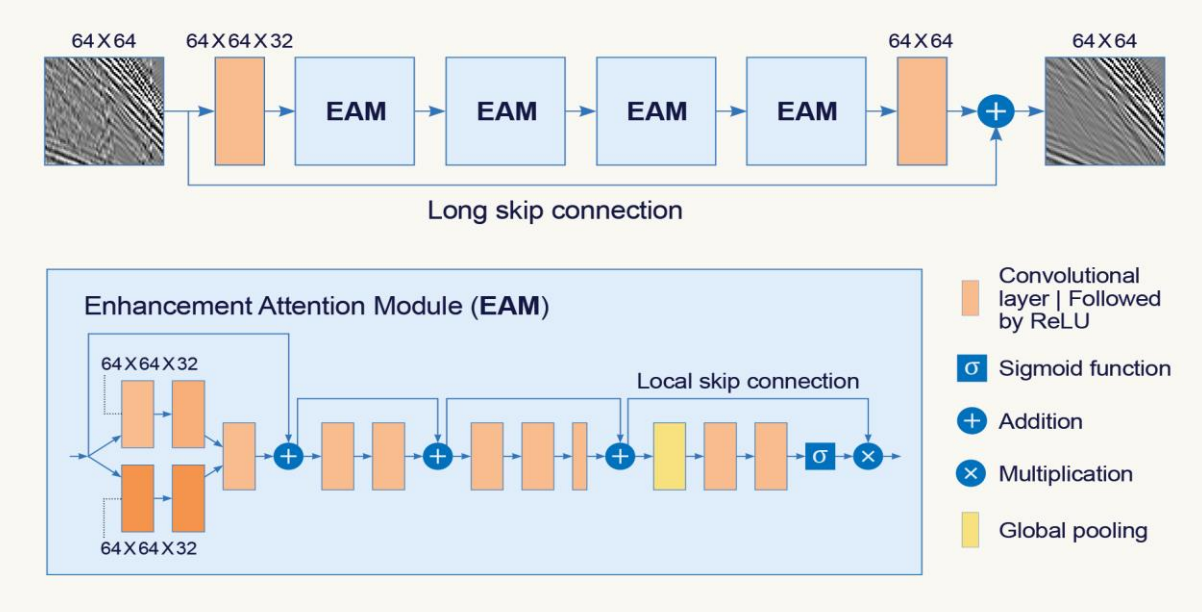

Figure 1 *Schematic of the RIDNet convolutional neural network architecture.*

To train a RIDNet model for noise attenuation of pressure data, we used noise attenuated data from the workflow proposed by Farmani and Pedersen (2022). Their workflow consists of three main elements: sample based deep learning classification using U-Net networks, FX deconvolution filters and FX projection filters. This workflow also runs in an automated fashion without user interaction, and it produces consistent noise attenuated outputs. As this workflow has been used in production for some time, a large body of noise attenuated pressure data was available to train the RIDNet model. We selected 660,000 tiles for training such that they cover a large variation of geology, water depth, input noise level and acquisition geometry. Our training could reach PSNR of 47.1 on validation data. Our pressure RIDNet model targets noise in pressure data below 25 Hz as most of the noise is at the lowest frequencies. Noise above 25 Hz, if present, is targeted using FX filters. Linear coherent noise is supressed by FK filters in the workflow.

Example

The data selected for this example were acquired using a dual-sensor streamer offshore Newfoundland, Canada. The water depth is approximately 1500-3200 m in the survey area. The data were acquired during summer 2022. Figures 2 shows shot gather examples for pressure records before and after the noise attenuation and attenuated noise. Figure 3 shows a part of 2D QC (Quality Control) stack from the same survey. The workflow attenuates the pressure record noise very effectively. Figures 4 and 5 show similar data recorded by particle motion sensors. Note how the nature of the noise is different between pressure and particle motion records. In this example, the noise recorded by the pressure sensors is mainly due to the environmental conditions and the noise recorded by the particle motion sensors is mainly due to the vibration noise caused by external devices attached to the streamer. Particle motion noise is rather strong on this example but is heavily supressed by the workflow. However, some residual noise can be observed particularly on near offsets. This level of residual noise does not affect the quality of the up-going pressure field and will be further supressed in the subsequent processing steps. The final product of multisensor acquisition is usually the up-going pressure field. Figure 6 shows the same shot gathers and 2D QC stack as in Figures 2 to 5 after generating the up-going wavefield. Note the low level of noise in the up-going wavefield.

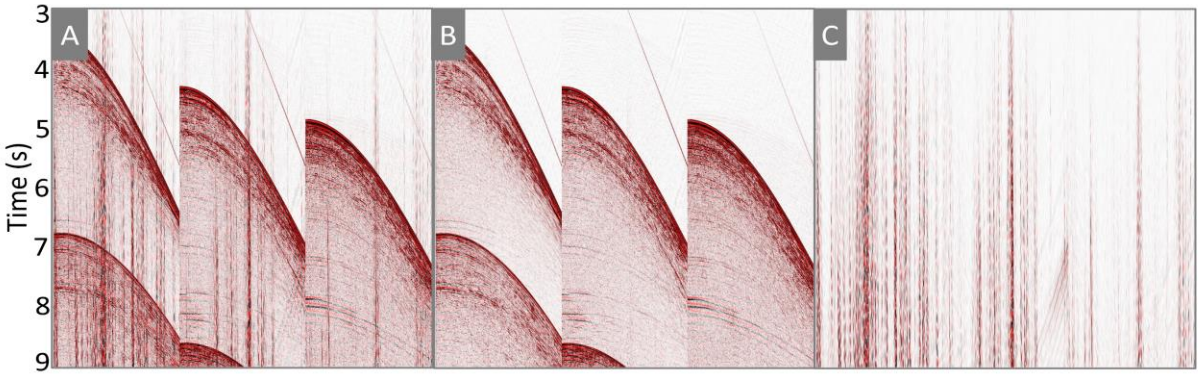

Figure 2 *Shot gather examples of hydrophone records a) before and b) after the noise attenuation. c) noise attenuated by the workflow.*

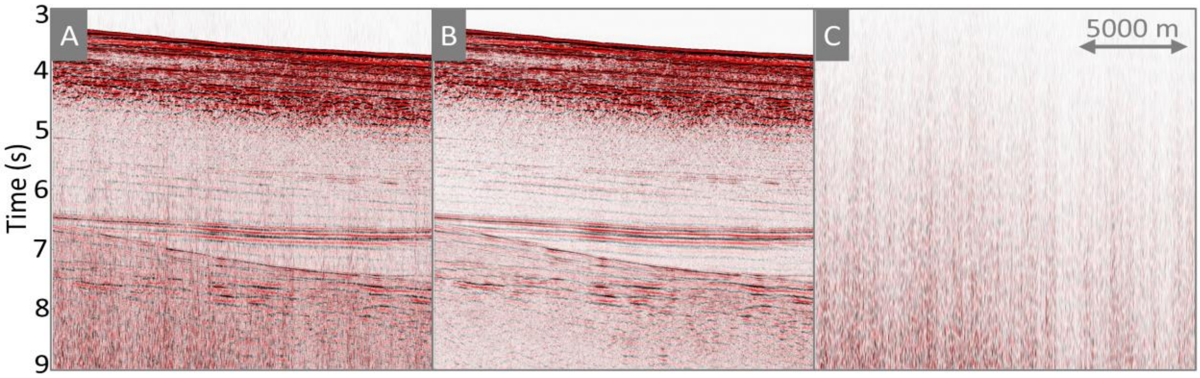

Figure 3 *2D QC stack of pressure records a) before and b) after the noise attenuation. c) noise attenuated by the workflow.*

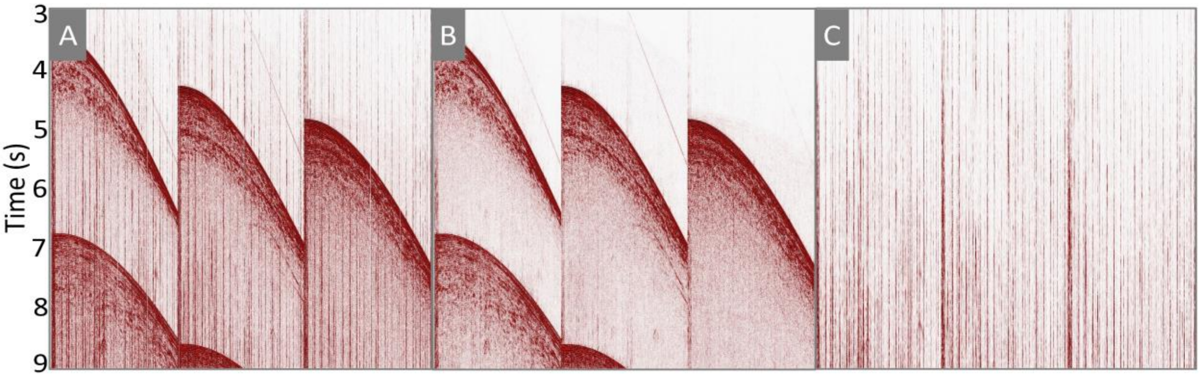

Figure 4 *Shot gather examples of particle motion records a) before and b) after the noise attenuation. c) noise attenuated by the workflow. A 20-30 Hz Ormsby lowcut filter was applied for display purposes.*

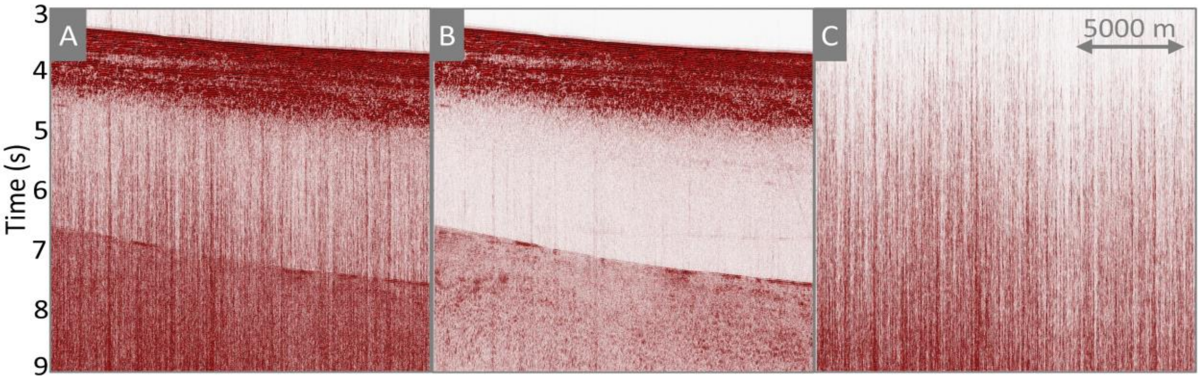

Figure 5 *2D QC stack of particle motion records a) before and b) after the noise attenuation. c) noise attenuated by the workflow. A 20-30 Hz Ormsby lowcut filter was applied to the input to the stacks.*

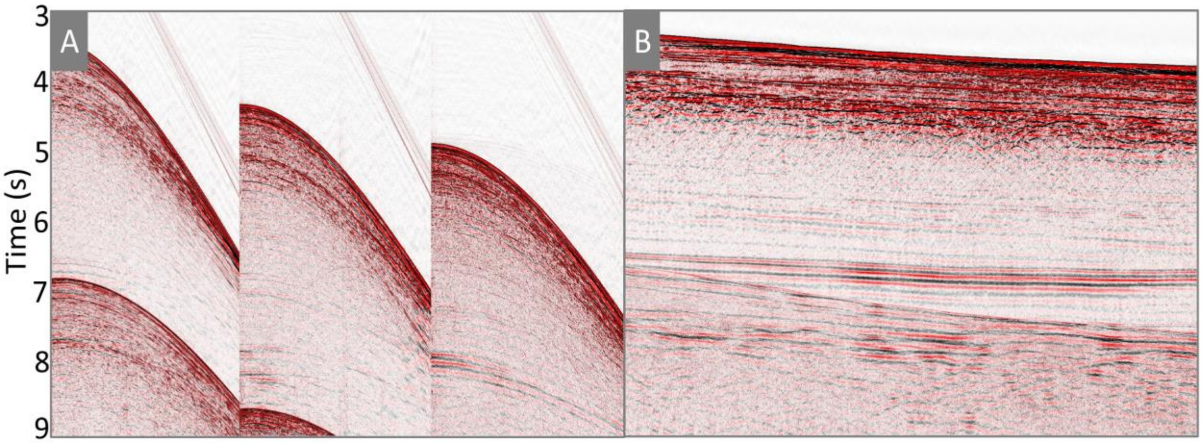

Figure 6 *Shot gather examples (a) and 2D QC stack (b) of the up-going pressure field generated from the noise attenuated pressure and particle motion records.*

Conclusions

Multisensor noise attenuation workflows have been designed to simplify and further improve the noise attenuation on both pressure and particle motion sensors. The network is based on convolutional layers using the RIDNet architecture. Both models were trained using data recorded in the field with supervised learning where the desired outputs were produced by previously developed machine learning based workflows. The new workflows have been extensively validated using records from surveys acquired with different survey geometry, water depth and sea conditions. The validation process confirms that there is no need for workflow modification or re-training of the models. Therefore, the workflows are automated and do not require user interaction. In common with previous machine learning based workflows that we have presented, the parameter testing phase necessary for the conventional noise attenuation approaches is eliminated. Depending on the hardware resource, the computational expense of the RIDNet-based workflows is less or comparable to machine learning based approaches that we have previously presented. Both workflows are available for the use in production.

Acknowledgements

We would like to thank PGS for the permission to publish these results.

References

Anwar, S., and Barnes, N. [2019]. Real Image Denoising with Feature Attention. *IEEE International Conference on Computer Vision (ICCV)*.

Bekara, M., and A. Day. [2019]. Automatic QC of denoise processing using a machine learning classification. *First Break*, 37 (9), 51-58.

Farmani, B. and Pedersen, M.W. [2022]. Stepping Towards Automated Multisensor Noise Attenuation Guided by Deep Learning. *83rd EAGE Annual Conference & Exhibition*, Jun 2022, Volume 2022, p.1-5.

Farmani, B., Pal, Y., Pedersen, M.W. and Hodges, E. [2023]. Motion sensor noise attenuation using deep learning. *First Break*, 41 (2), in press

Kumar, A., Dancer, K., Rayment, T., Hampson, G. and Burgess, T. [2022]. Deep Learning Swell Noise Estimation. *First Break*, 40 (9), 31-36.

Valenciano, A., Brusova, O., and Cheng, C. [2022]. Efficient Swell Noise Removal Using a Global Deep Neural Network Model. *First Break*, 40 (2), 51-55.